Project Number: [956004]
Project Acronym: [BioTrib]
Project title: [**Advanced Research Training for the Biotribology of Natural and Artificial Joints in the 21st Century**]

Quantitative characterisation of AM bearing surfaces

Deliverable D3.3

Month Due: PM22

Month Delivered: PM23

Project coordinator name	Prof. Richard M Hall
Project coordinator organisation name	UNIVLEEDS
Report prepared by	Qingyue Shi Jules Barot Dr Connor Myant Dr Rob Hewson Prof Richard M Hall Review by members of the Supervisory Board

Dissemination Level of Report

PU	Public	X
PP	Restricted to other program participants (including the Commission Services)	
RE	Restricted to a group specified by the consortium (including the Commission Services)	
CO	Confidential, only for members of the consortium (including the Commission Services)	

The BioTrib ETN project has received funding from the European Union's Horizon 2020 research and innovation programme under grant agreement No. 956004.

BioTrib

Deliverable Number: D3.3

Quantitative Characterisation of AM Bearing Surfaces: Preliminary Results

ESR 10
Qingyue Shi

Research Title:
Tribology of 3D Printed Prostheses

Supervisors:
Dr Connor Myant, Dr Robert Hewson

Imperial College London

This project has received funding from the European Union's Horizon 2020 research and innovation programme under the Marie Skłodowska-Curie grant agreement No 956004

Table of Contents

1) Introduction

Selective laser melting (SLM) is a 3D printing technique commonly employed for metals. SLM systems utilise a powder bed feedstock and a laser energy source to fuse the metal particles locally, layer by layer in a sequential additive pattern.[1] This is in stark contrast to traditional manufacturing techniques such as casting, where parts are typically created in one global step (e.g., molten metal poured in a mould and left to cool). This difference in manufacturing processes means parts undergo considerably different thermal conditions; SLM parts experience local, rapid, repetitive heating and cooling cycles, while traditional parts experience single, global, cooling patterns. SLM has a much higher cooling rate in the range of 10^4-10^6 Ks^{-1} compared to the conventional casting process (~102 Ks-1).[2], [3] The rapid cooling rate in SLM results in small grain sizes and high dislocation densities that promote the yield strength of SLM fabricated materials by boundary strengthening mechanisms.[4], [5] Thus, tribological properties have been found distinct in parts fabricated by SLM compared to ones cast. [4], [6] However, the detailed characterization of the wear behaviour of SLM parts and the impact of their microstructure on their wear resistance is not well documented. Although several variables have been investigated, a connection between the microstructure and the resultant tribological behaviour is still required. As can be observed, it might be fascinating to continue identifying the best technique to manage the grain structure using the machine's parameters and see whether it can affect the wear rate. This will be a goal for this research project: to improve the wear resistance of SLM metals.

Preliminary tests have been carried out to study the effect of the scanning direction of unidirectional scan strategies on the wear behaviours of 316L stainless steel, and demonstrate the ability to characterise 3D printed metal bearing surfaces.

2) Methods

a. Sample Fabrication

The 3D models of specimens are designed in CAD software (Fusion 360, Autodesk) and exported as STL files. The specimens were printed using SLM 3D printer Concept Mlab CUSING with a laser power of 90 W, scanning speed of 600 mm/s, hatch spacing of 77 μm, and layer thickness of 25 μm in an argon atmosphere. These process parameters were chosen to achieve minimum porosity as suggested by the manufacturer. Disc specimens were printed with 316L stainless steel with a diameter of 3.5 mm and a height of 10 mm. A notch was designed in the specimen and printed to identify the scanning direction so that the wear tests can be done aligning with it or being perpendicular to it, as shown in Figure 1. The metal powder used in this study was 316L stainless provided by LPW Technology. Bulk 316L stainless steel samples are also made by cutting the 316L steel bars into discs to compare with the SLM 316L steel samples.

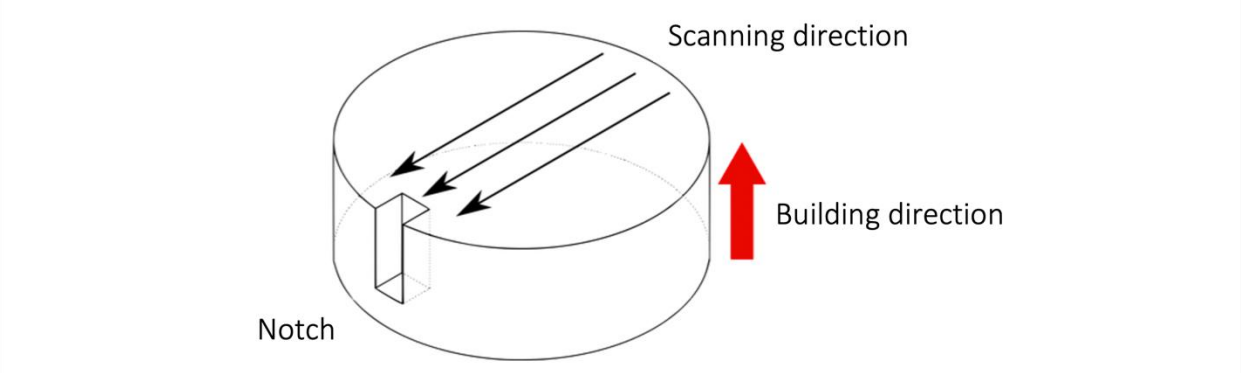

Figure 1 Illustration for the 3D-printed sample with a notch indicating the laser scanning direction

b. Sample Preparation

Samples are polished to a mirror finish with grit cloth and diamond suspension to 0.04 μm on a Labopol-21 from Struers. The ball and sample were cleaned in an ultrasonic bath of isopropanol to remove residuals or grease to ensure the repeatability of wear tests.

c. Wear Test and Measurement

A high-frequency linear reciprocating rig (HFRR) from PCS-Instruments was used for the tribological test in dry conditions at room temperature. Stainless steel balls (diameter = 6 mm) will be used to rub on the flat surface with a stroke length of 1.5 mm at a frequency of 50 Hz for 30 min. Normal loads from 100 g to 500 g were applied, as illustrated in Figure 2 showing the HFRR principle.

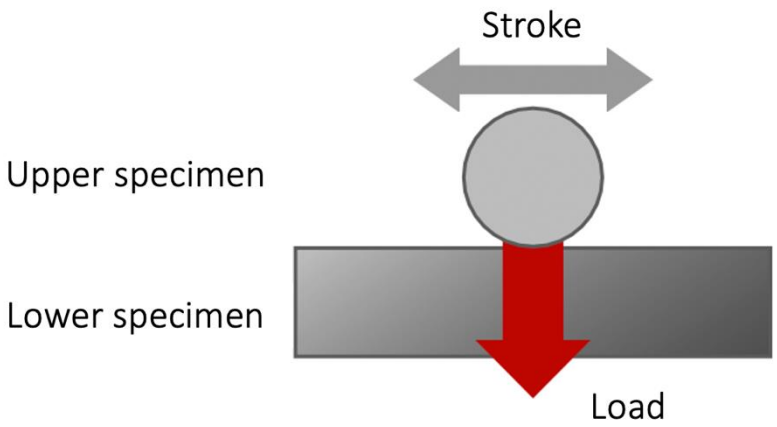

Figure 2 The HFRR principal

The material used for the upper specimen was 316L stainless steel and the lower specimens are 3D-printed and bulk 316L stainless steel discs. Two sliding directions were tested as aligned with the scanning direction (Figure 3 (a)), and perpendicular to the scanning direction (Figure 3 (b)).

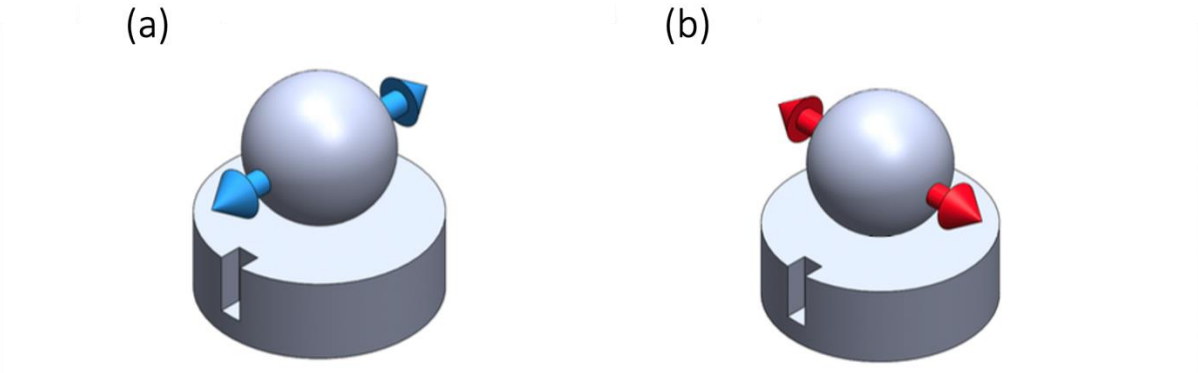

Figure 3 Schematics of the sliding directions: (a) Sliding direction aligned with scanning direction; (b) Sliding direction perpendicular to scanning direction.

The friction force was measured by the transducer and plotted in real-time and the friction coefficient is measured by dividing the friction force by the load used during the test. The friction coefficient was measured and averaged during the last 5 minutes of the test to make sure the stationary regime is reached. Three replicates of each sample type were tested for each test. The coefficient of friction (COF) value is calculated by averaging the three tests, and the error at 95% was also calculated.

Specimens were cleaned in the sonicated bath for wear tracks examination after the sliding tests. The wear track was measured by motorized white light interferometry (WLI) with Veeco (Ref Wyko NT9100) and the wear volume will be calculated based on the total displaced volume. The two wear profiles of the cross sections of the wear scar (ZX which is the profile perpendicular to the sliding direction, and ZY which is in line with the sliding direction) were obtained. An example wear track is presented in Figure 4. To calculate the volume lost, the wear scar is estimated as a half ellipsoid with the semi-principal axes a, b and c measured from the scar profiles as shown in Figures 4 b and c. Thus, the volume lost is calculated by $\frac{2}{3}\pi abc$.

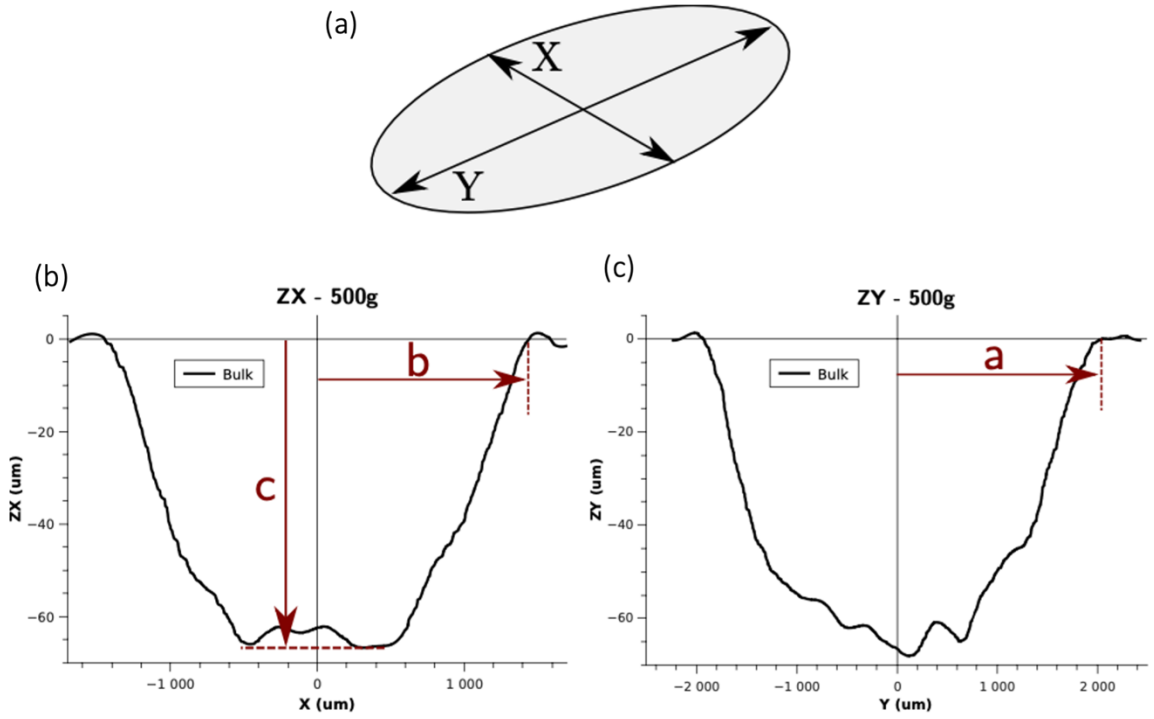

Figure 4 (a) Schematic of the cross-section profiles perpendicular to (X) and in line with the sliding direction (Y); (b, c) example wear scar profiles in X and Y directions.

The wear rate (mm^3/m) is then calculated as volume (mm^3) divided by the and the total distance (m):

$$Wear\ rate = \frac{Volume}{Total\ distance}$$

The mass loss is measured by comparing the weight of the ball and specimen before and after the sliding tests. The ball and specimen were thoroughly cleaned before weighting by a weighting scale from Sartorius.

3) Results and Discussion

a. Friction Coefficient

The coefficient of friction (COF) of bulk samples and 3D-printed samples tested in two sliding directions (AM-90d as perpendicular to and AM-0d as aligned with the scanning direction) are shown in Figure 5. The error bars show the 95% confidence interval around the mean values.

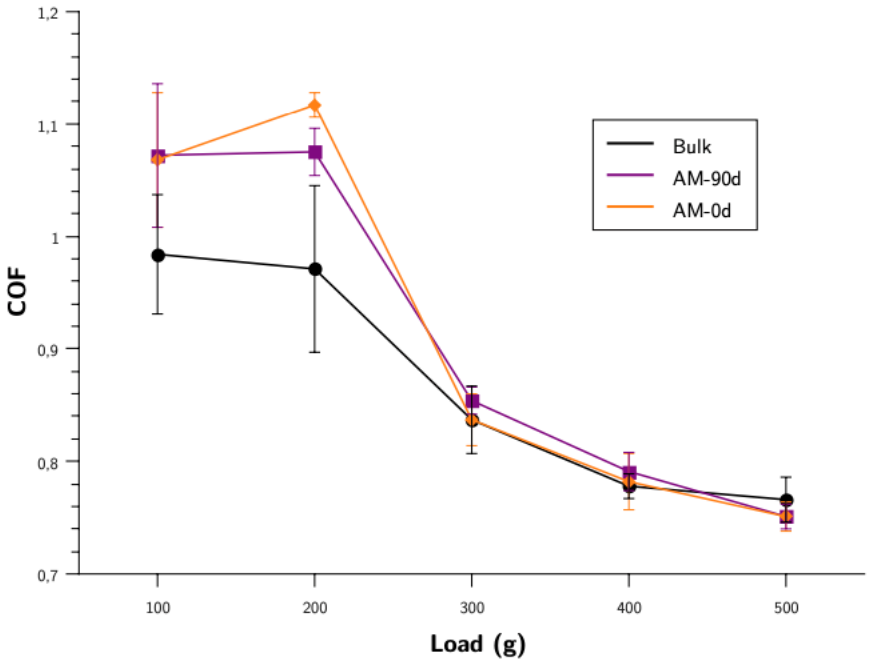

Figure 5 Friction coefficient curves for AM and bulk material

The three types of tested samples all follow a similar trend in that the COF decreases with high loads before stabilizing for higher loads. Bulk material provides a lower friction coefficient with a reduction of around 10% while under low loads (less than 300 g). No matter the wearing direction in relation to the printing direction, friction curves merge at high loads, indicating that there is no significant difference in friction coefficient between bulk and 3D-printed 316L. Because friction curves for 3D-printed samples can be viewed as combined for all loads, the effect of sliding direction with respect to the scanning direction has no significant impact on the COF.

b. Wear Scar Profiles

From the wear scar profiles of both X and Y cross sections, the bulk sample is observed to have on average smaller wear scars than 3D-printed samples at low loads but larger at high loads, shown in Figure 6 as examples of wear scars at the load of 100 g and 500 g. As the wear surfaces were rough, the middle line of the wear scar is not always the deepest, so X profiles were preferred to compare between samples instead of Y profiles. In Figure 7- 9, the X profiles are compared for samples under different loads. The X profiles (Figure 7) of bulk samples seemed to have two regimes for high loads (400 g and 500 g) and low loads (300 g under). While this phenomenon was not observed for 3D-printed samples worn in two sliding directions, where the wear behaviours seem more linear (Figure 8&9). Wear volume has been assessed using the ellipsoid approximation to confirm these observations from the wear scar profiles.

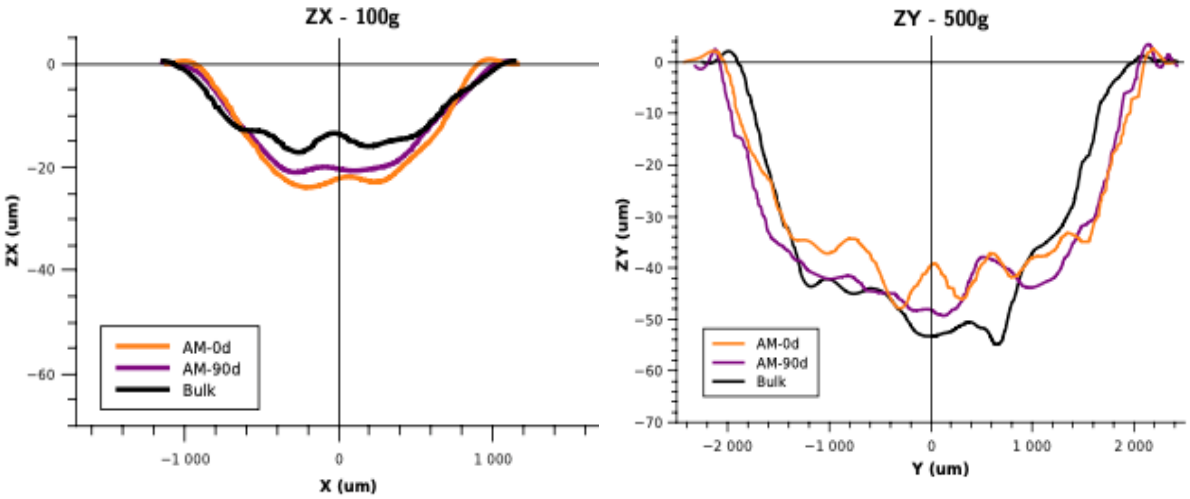

Figure 6 Examples of wear scars at the load of 100 g and 500 g.

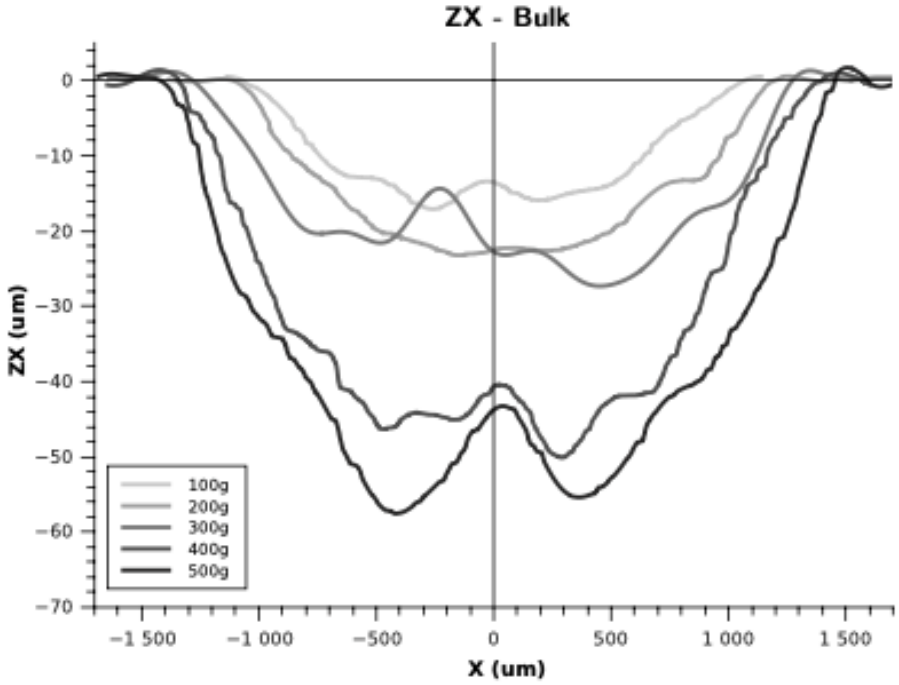

Figure 7 Averaged ZX Wear Scar Profiles for Bulk Samples

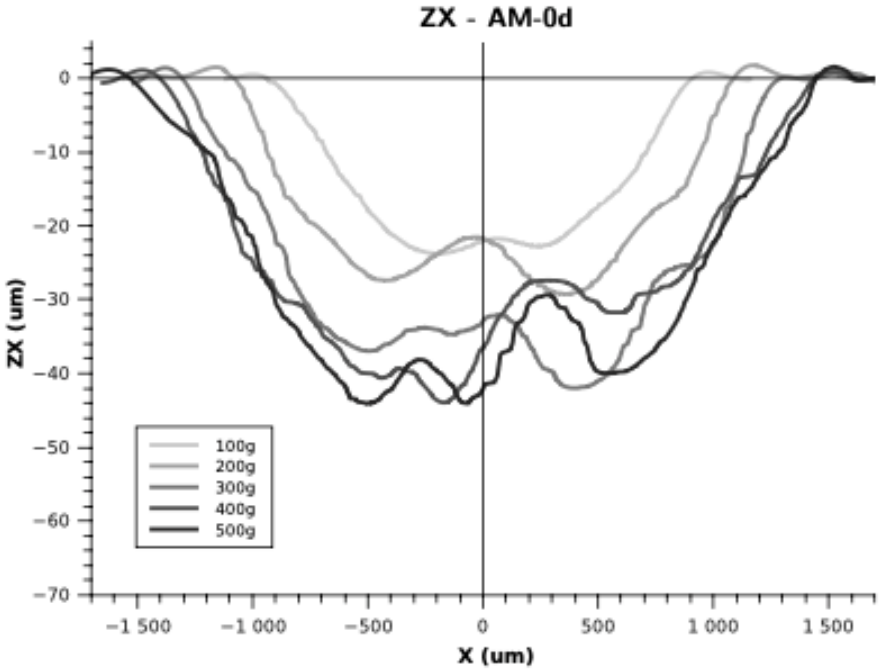

Figure 8 Averaged ZX wear scar profiles for the 3D-printed sample with the aligned sliding direction

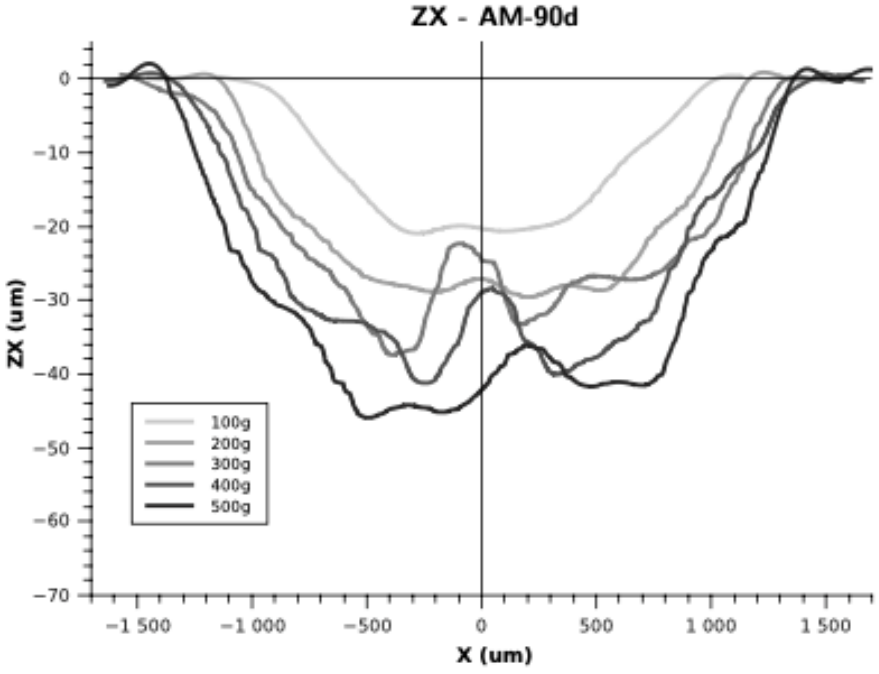

Figure 9 Averaged ZX wear scar profiles for the 3D-printed sample with the perpendicular sliding direction

c. Wear volume

Figure 10 presents the wear volume for both materials and two sliding directions. It can be seen that it increases with load indicating that the wear conditions are worse and causing more wear with higher loads. For 3D-printed samples, a linear variation is shown. The two sliding directions yield the same trends and curves. Bulk samples exhibit two distinct regimes, one at low loads (less than 300 g) and the other at larger loads, while both appear to change linearly. This trend for bulk samples can be related to the two-regime observed in wear scar profiles.

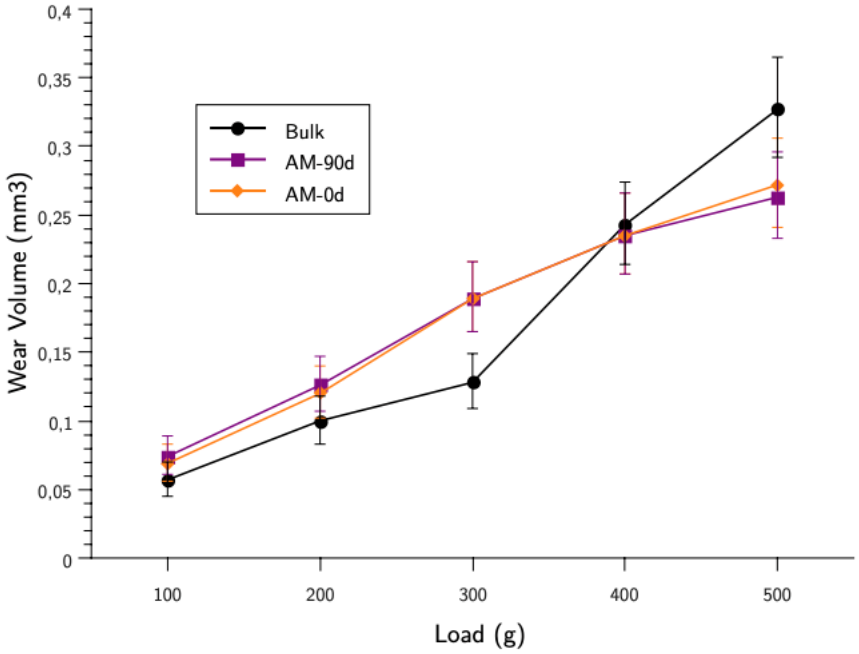

Figure 10 Wear volumes of samples on different loads

d. Mass loss

As shown in Figure 11&12 mass losses of the ball and the disc under different loads. The current patterns are consistent with earlier ones in wear scar profiles and volume loss: the mass loss of bulk samples appears to have two wear regimes depending on the load applied, and 3D-printed samples exhibit linear wear behaviour with loads. The two curves (AM-0d and AM-90d) for 3D-printed samples worn with a wear stroke aligned with and perpendicular to the scanning direction are combined, correlating to the pattern found in wear volume. While the mass loss of the ball showed no significant difference among bulk samples and 3D-printed samples.

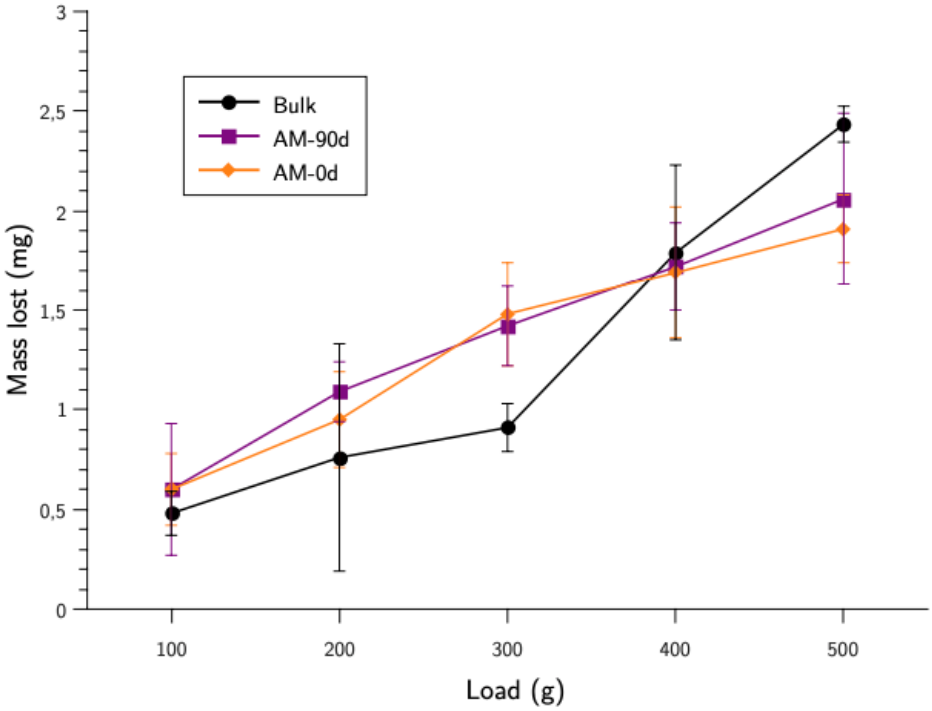

Figure 11 Mass loss of samples on different loads

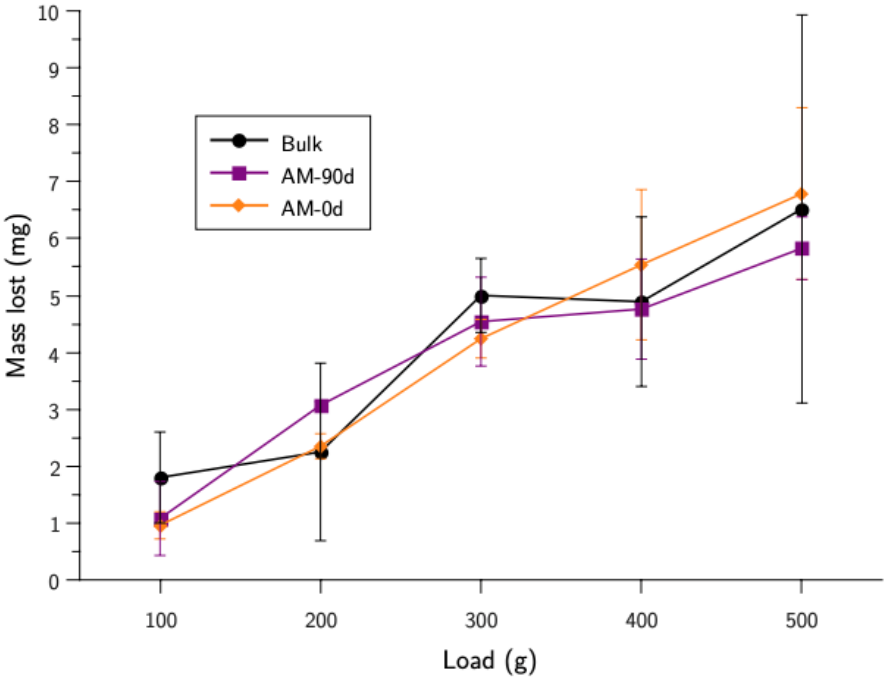

Figure 12 Mass loss of balls on different loads

To confirm the consistency found between the wear volume and mass loss, the correlation of these two characteristics of wear behaviours is plotted in Figure 13. For all 3 types of samples, the mass lost and the volume lost have linear correlation which means both methods are relevant. The two

regimes of wear behaviours under high loads and low loads of bulk samples are also observed here, which indicated a switch from a mild wear regime to a more severe one.

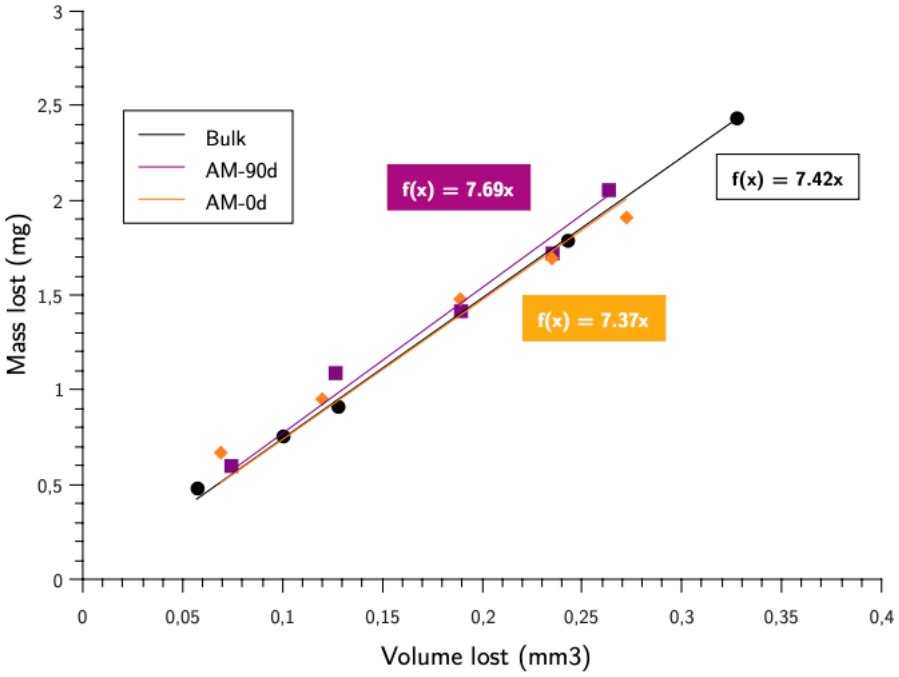

Figure 13 Correlation between volume lost and mass lost of samples

4) Conclusion

The tribological properties of 3D-printed 316L stainless steel have been examined in this study and compared with bulk material. 3D-printed samples have been worn in dry sliding with a wear stroke that is parallel to or perpendicular to the printing direction after being printed using a unidirectional scanning strategy. Based on the results, conclusions are made as follows:

- It is possible to carry out indepth tribological analysis of 3D printed bearing surfaces.
- 3D-printed material has a higher friction coefficient than bulk material at low loads, but once a severe wear regime is reached, they behaved similarly.
- For unidirectional 3D-printed samples, where the surface being worn is in a plane perpendicular to the building direction, the wear direction has no significant impact on the friction coefficient or the wear behaviour.

5) References

[1] T. Larimian, B. AlMangour, D. Grzesiak, G. Walunj, and T. Borkar, “Effect of Laser Spot Size, Scanning Strategy, Scanning Speed, and Laser Power on Microstructure and Mechanical Behavior of 316L Stainless Steel Fabricated via Selective Laser Melting,” *J Mater Eng Perform*, Nov. 2021, doi: 10.1007/s11665-021-06387-8.

[2] P. K. Gokuldoss, S. Kolla, and J. Eckert, “Additive manufacturing processes: Selective laser melting, electron beam melting and binder jetting-selection guidelines,” *Materials*, vol. 10, no. 6. MDPI AG, 2017. doi: 10.3390/ma10060672.

[3] S. W. Xu, K. Oh-ishi, S. Kamado, H. Takahashi, and T. Homma, “Effects of different cooling rates during two casting processes on the microstructures and mechanical properties of extruded Mg-Al-Ca-Mn alloy,” *Materials Science and Engineering A*, vol. 542, pp. 71–78, Apr. 2012, doi: 10.1016/j.msea.2012.02.034.

[4] N. Hansen, “Hall-petch relation and boundary strengthening,” *Scr Mater*, vol. 51, no. 8 SPEC. ISS., pp. 801–806, 2004, doi: 10.1016/j.scriptamat.2004.06.002.

[5] V. Kumar, M. D. Joshi, C. Pruncu, I. Singh, and S. S. Hosmani, “Microstructure and Tribological Response of Selective Laser Melted AISI 316L Stainless Steel: The Role of Severe Surface Deformation,” *J Mater Eng Perform*, vol. 30, no. 7, pp. 5170–5183, Jul. 2021, doi: 10.1007/s11665-021-05730-3.

[6] W. L. Li, N. R. Tao, Z. Han, and K. Lu, “Comparisons of dry sliding tribological behaviors between coarse-grained and nanocrystalline copper,” *Wear*, vol. 274–275, pp. 306–312, Jan. 2012, doi: 10.1016/j.wear.2011.09.010.